

Wavelet Methods for Optical Surfaces - Representation, Analysis and Simulation

Philipp Jester^{*/**}, Christoph Menke^{*}, Karsten Urban^{**}

^{*}Carl Zeiss AG, Oberkochen

^{**}Institute of Numerical Mathematics, Ulm University

mailto:p.jester@zeiss.de

Wavelets are well adapted to describe local and global structures and so lead to an alternative surface representation that combine a high approximation accuracy with a fast evaluation. We show that this new representation is usable in a ray tracing algorithm and can be used to analyse surface data.

1 Introduction

In optics, common optical surfaces are well described in terms of a power series expansion or even simpler descriptions. These representations turn out to be impractical in some cases, like for freeform surfaces or aspheric surfaces including manufacturing errors. An alternative surface representation is given by wavelets.

2 B-Spline and Wavelet Representation

We focus on smooth optical surfaces potentially with some local defects, so choosing *cardinal B-splines* as basis functions seems promising. Therefore locality and recursion are well-known and essential for a fast evaluation of the representation. One can show that a refinement equation holds, this enables B-splines to generate a *Multiresolution Analysis* (MRA), see [1] and [2].

So, we fix φ a B-spline of order d and use it as scaling function of our MRA. The properties of a MRA then imply the existence of a dual scaling function $\tilde{\varphi}$, such that

$$(\varphi(\cdot), \tilde{\varphi}(\cdot - k))_{L_2(\mathbb{R})} = \delta_{0,k}, \quad k \in \mathbb{Z},$$

holds.

For a piecewise continuous function $g : \mathbb{R} \rightarrow \mathbb{R}$ we denote by $g_{j,k}(x) := 2^{j/2}g(2^jx - k)$ a scaled and shifted variant. Using this notation we define the biorthogonal projection $P_j : L_2(\mathbb{R}) \rightarrow S_j$ of a function $f \in L_2(\mathbb{R})$ onto the space $S_j := \text{clos}_{L_2(\mathbb{R})}\{\varphi_{j,k} : k \in \mathbb{Z}\}$ by

$$P_j f = \sum_{k \in \mathbb{Z}} (f, \tilde{\varphi}_{j,k})_{L_2(\mathbb{R})} \varphi_{j,k}. \quad (1)$$

The dual space \tilde{S}_j is defined in a similar way.

Here, we want to introduce wavelets. Let W_j, \tilde{W}_j be the complement spaces, such that

$$\begin{aligned} S_{j+1} &= S_j \oplus W_j, & S_j &\perp \tilde{W}_j, \\ \tilde{S}_{j+1} &= \tilde{S}_j \oplus \tilde{W}_j, & \tilde{S}_j &\perp W_j, \end{aligned}$$

holds. A function ψ is called *primal wavelet* if $\{\psi_{j,k} : k \in \mathbb{Z}\}$ is a Riesz basis for W_j . The corresponding

dual wavelet is denoted by $\tilde{\psi}$.

Now, we get an equivalent representation for our projection in terms of wavelets

$$P_j f = \sum_{\ell=-1}^{j-1} \sum_{k \in \mathbb{Z}} (f, \tilde{\psi}_{j,k})_{L_2(\mathbb{R})} \psi_{j,k}. \quad (2)$$

Defining the coefficients $c_{j,k} := (f, \tilde{\varphi}_{j,k})_{L_2(\mathbb{R})}$ and $d_{j,k} := (f, \tilde{\psi}_{j,k})_{L_2(\mathbb{R})}$ the *Fast Wavelet Transform* maps the vector $\mathbf{c}_j := (c_{j,k})_k$ to $\mathbf{d}_j := (d_{j,k})_k$,

$$\text{FWT} : \mathbf{c}_j \mapsto (\mathbf{c}_0, \mathbf{d}_0, \dots, \mathbf{d}_{j-1}).$$

The FWT is of linear complexity as long as primal and dual scaling functions are compactly supported. Two dimensional scaling functions and wavelets are constructed by the bivariate tensor product. We are now ready to describe and analyse optical surfaces with wavelets.

3 Accuracy

First, we have to show that the projection in equation (1) can be used in a ray tracing algorithm with sufficient accuracy. The following error estimate is well-known for a function $f \in H^s(\mathbb{R})$, $0 \leq s \leq d$,

$$\|f - P_j f\|_{L_2(\mathbb{R})} \leq C_1 \cdot 2^{-js} \|f\|_{H^s(\mathbb{R})}, \quad C_1 > 0.$$

We need to compute the coefficients $c_{j,k}$. This can not be done directly, because there is no analytic form for the dual scaling function available. Instead we use the following quasi-interpolation scheme

$$c_{j,k} \approx \bar{c}_{j,k} := 2^{j/2} \sum_{\ell=-m}^m \gamma_{d,\ell} f(2^{-j}(k + \ell))$$

with $m := \lfloor \frac{d-1}{2} \rfloor$ and weights $\gamma_{d,\ell}$, see [3], [4]. The quasi-interpolant

$$\bar{P}_j f := \sum_{k \in \mathbb{Z}} \bar{c}_{j,k} \varphi_{j,k}$$

is of the same order of approximation as P_j , in particular one gets

$$\|f - \bar{P}_j f\|_{L_2(\mathbb{R})} \leq C_2 \cdot 2^{-js} \|f\|_{H^{-s}(\mathbb{R})}, \quad C_2 > 0.$$

An aspheric surface is used to test the above method. For $n = 10^6$ rays, we report the maximal deviation of intersection points calculated with respect to our method $\mathbf{x}_i^{(j)}$ and the usual representation $\mathbf{x}_i^{(O)}$, i.e.

$$M_j := \max_{i=1, \dots, n} \{ \|\mathbf{x}_i^{(O)} - \mathbf{x}_i^{(j)}\| \}.$$

Figure 1 shows an error plot for different B-spline orders $d = 2, \dots, 6$. The accuracy of the ray tracing is fixed to $\varepsilon = 10^{-12}$.

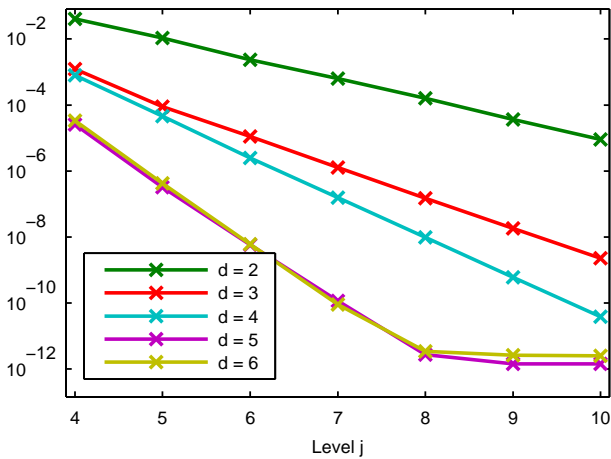


Fig. 1 Maximal deviation M_j of intersection points.

We see that an approximation accuracy up to the desired tolerance is reached for orders $d = 5, 6$ and level $j \geq 8$.

4 Wavelet Analysis

Next, we describe the use of wavelet methods to analyse given real and synthetic optical surfaces. For the detection of local errors we add an artificial perturbation to a measured aspheric surface. The resulting surface is shown in the left part of Fig. 2.

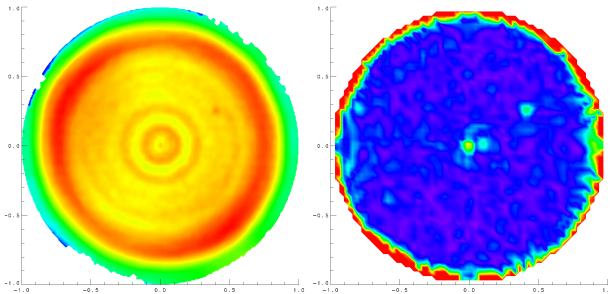


Fig. 2 Surface with artificial error (left) and combined wavelet detail for level $j = 6$ (right).

The combined wavelet detail of level $j = 6$ is shown in the right part of Fig. 2, where we define the combined wavelet detail by the element-wise euclidean norm of horizontal, vertical and diagonal detail. The

local perturbation is clearly visible in the wavelet decomposition at position $(0.4, 0.25)$. One notices also a true error in the mid of the surface.

Finally we use wavelets to localize mid spatial frequency perturbed domains. Therefore we split our surface in outer and inner domain and add artificial errors, modelled by a *Power Spectral Density* function, with different intensities to each domain. To get a more realistic model we also add a low spatial frequency error in terms of Zernike polynomials. An example is shown in the left part of Fig. 3.

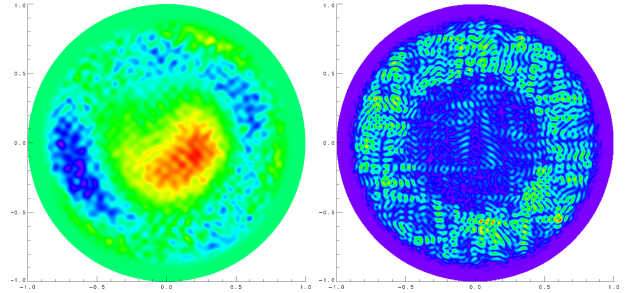


Fig. 3 Surface with domains of varying PSD-errors (left) and combined wavelet details for level $j = 9$.

The combined wavelet detail in the right part of Fig. 3 clearly shows the differing domains.

5 Summary

The presented wavelet method can be used to approximate an optical surface up to machine accuracy. This representation is usable in a ray tracing algorithm.

Furthermore we used wavelets to analyse and detect errors of optical surfaces. Single local errors are detected as well as domains of differing errors. We think the presented results show a broad field of application of wavelets in optics.

References

- [1] C. de Boor, *A practical guide to splines*, vol. 27 of *Appl. Math. Sci.*, revised ed. (Springer-Verlag, New York, 2001).
- [2] A. Cohen, I. Daubechies, and J.-C. Feauveau, "Biorthogonal bases of compactly supported wavelets," *Comm. Pure Appl. Math.* **45**(5), 485–560 (1992).
- [3] V. A. Zheludev, "Local quasi-interpolation splines and Fourier transforms," *Dokl. Akad. Nauk SSSR* **282**(6), 1293–1298 (1985).
- [4] K. Bittner and K. Urban, "Adaptive wavelet methods using semiorthogonal spline wavelets: sparse evaluation of nonlinear functions," *Appl. Comput. Harmon. Anal.* **24**(1), 94–119 (2008).
- [5] P. Jester, C. Menke, and K. Urban, "Wavelet Methods for the Representation, Analysis and Simulation of Optical Surfaces," to appear.